Smart Timber Bridge on Geosynthetic Reinforced Soil (GRS) Abutments

Adam Senalik
Research Engineer
Forest Products Laboratory
Madison, WI, USA
christopherasenalik@fs.fed.us

Adam is a recent graduate of the University of Illinois, Urbana-Champaign, where his PhD thesis focused on nondestructive inspection of glulam beams. He has worked at FPL in timber bridge research for 4 years on a wide variety of projects.

James P. Wacker
Research Engineer
Forest Products Laboratory
Madison, WI, USA
jwacker@fs.fed.us

James completed his Civil and Environmental Engineering studies at the University of Wisconsin – Madison. His FPL research has primarily been focused on timber bridge-related studies for the past 27 years. He is also a registered professional engineer in the state of Wisconsin.

Travis K. Hosteng
Director/Engineer
National Center for Wood Transportation Structures
Ames, IA, USA
kickhos@iastate.edu

Travis earned his MSc degree from Iowa State University. He is the lead engineer for wood bridge projects at ISU's Bridge Engineering Center and Co-Director of the National Center for Wood Transportation Structures. He is a member on the ASCE committee for timber bridges.

John Hermanson
Research Scientist
Forest Products Lab.
Madison, WI, USA
jhermanson@fs.fed.us

John's research focuses on the areas of multifield and multidomain modelling of continuum systems.

Summary

Recently, Buchanan County, Iowa, has cooperated with the U.S. Federal Highway Administration (FHWA), USDA Forest Service, Forest Products Laboratory (FPL), and Iowa State University's Bridge Engineering Center (ISU–BEC) to initiate a project involving the construction and monitoring of a glued-laminated (glulam) timber superstructure on geosynthetic reinforced soil (GRS) integrated bridge system (IBS) abutments. The research team from FPL installed sensors in the substructure as well as in the bearings of the girders. In addition, the research team from ISU–BEC installed sensors on the superstructure that create an autonomous structural health monitoring system for the bridge. Data are collected remotely and transmitted continuously around the clock

every day. Long-term monitoring enables researchers to evaluate GRS–IBS system performance with respect to variables of time, ambient conditions, and loading.

Keywords: Geosynthetic reinforced soil, health monitoring, timber, glulam, substructure, superstructure

1. Introduction

In October 2016, the Catt bridge project was dedicated near the city of Independence in Buchanan County, Iowa, USA (42.475702° N, 91.828430° W) (Fig. 1). Its unique construction techniques were documented through a live webcam, which is accessible from the National Center for Wood Transportation Structures website (www.woodcenter.org). Buchanan County has a long history of constructing timber bridges, and it currently maintains 21 within its mostly rural, agriculture-based roadway network. Within the entire state of Iowa, there are approximately 3,000 timber bridges, the highest state inventory in the United States [1].

(a) (b)

Fig. 1 August 2016 photographs of the completed Catt Bridge: (a) End view (b) Profile view

Because it was one of the first timber bridge superstructures to be installed on geosynthetic reinforced soil (GRS) abutments in the United States, it provided the opportunity to collect key performance data using an array of sensors integrated into a structural health monitoring (SHM) system. The process of monitoring smart timber bridges is described in Phares et al. [2]. This project is a joint effort between the USDA Forest Products Laboratory (FPL), Iowa State University's Bridge Engineering Center (ISU–BEC), and the Federal Highway Administration (FHWA). This paper provides an overview of the design and construction phases, installation of sensors for SHM of the substructure and superstructure systems, and a review of the preliminary monitoring data collected to date.

2. Substructure Design

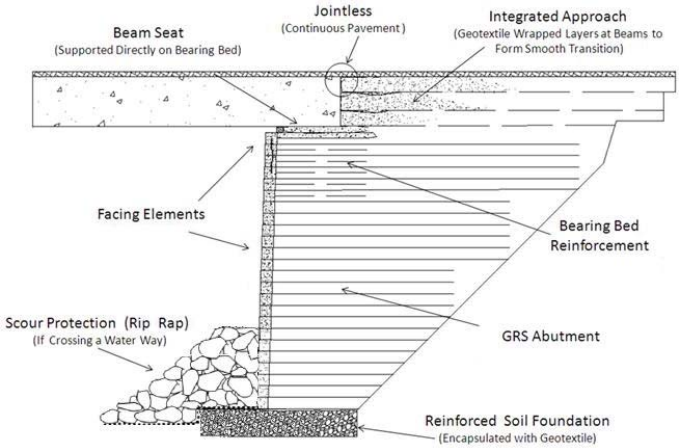

Fig 2. Geotextile reinforced soil integrated bridge system cross section showing typical characteristics (Used with the permission of FHWA)

As part of the Bridge of the Future Initiative, FHWA developed the GRS integrated bridge system (IBS). Geosynthetic reinforced soil walls (originally referred to as Geotextile-reinforced walls) were first constructed by the U.S. Forest Service in 1974. The GRS–IBS uses reinforced soil as part of an economical bridge system. The GRS–IBS was developed to be lower cost, be faster to construct, have improved durability compared with other single-span bridge construction, and have design flexibility allowing for adaptation in the field. Typically, steel and concrete bridge superstructures have been used with GRS–IBS. The bridge superstructure of a GRS-IBS is set

directly on the GRS abutment, which provides a stable foundation without the need for deep foundations or cast-in-place concrete. Prior to the construction of this bridge, only one timber bridge superstructure was known to be built on a GRS–IBS substructure.

A GRS–IBS cross section is shown in Figure 2, with typical characteristics identified. The GRS was built using a layered construction of aggregate wrapped in geotextile fabric. The fill material met Processed Aggregate Size No. 89 [3] and was 13 mm or smaller. The fabric was a woven polypropylene geotextile sold as Geotex® 350ST (Propex, Chattanooga, TN) and met AASHTO M288 standards [4]. Construction is described in Adams et al. [5]. Deciding layer thickness is a part of the design process. For the subject bridge in this study, the deepest layers were the thickest at 200 mm. The layers within the bearing bed reinforcement were 100 mm. The layers beneath the integrated approach were 150 mm. Some key characteristics were the reinforced soil foundation, the GRS abutment, the bearing bed reinforcement on which the beam seat sits, and an integrated approach to the bridge. The bridge superstructure sits directly on the bearing bed and is connected to the roadway by in integrated approach. This construction creates a jointless, continuous pavement between the approach and the bridge. The entire GRS–IBS is designed such that the superstructure and the approach settle at the same rate, avoiding the development of a “bridge bump” where the approach meets the superstructure.

3. Superstructure Design

The bridge superstructure was made up of a traditional glulam stringer and transverse glulam panel deck system, a commonly constructed prefabricated bridge system (Fig. 3). The design was based on the current standards set forth by the American Association of State Highway Transportation Officials–Load and Resistance Factor Design (AASHTO–LRFD) specifications [6]. A total of six glulam bridge girders were spaced at 1.57 m (center-to-center), which were interconnected by 1.35-m-wide and 13-cm-thick diaphragms. The 17.1-cm-thick transverse glulam deck was comprised of 1.22-m-wide panels along the traffic direction. The glulam panels were edge-butted and interconnected with 13.1-cm-deep glulam stiffener beams that were through-bolted to the bottom side of the deck panels. The bridge spans 16.2 m between the GRS–IBS bridge abutments. The roadway measures 8.5 m between glulam bridge railings.

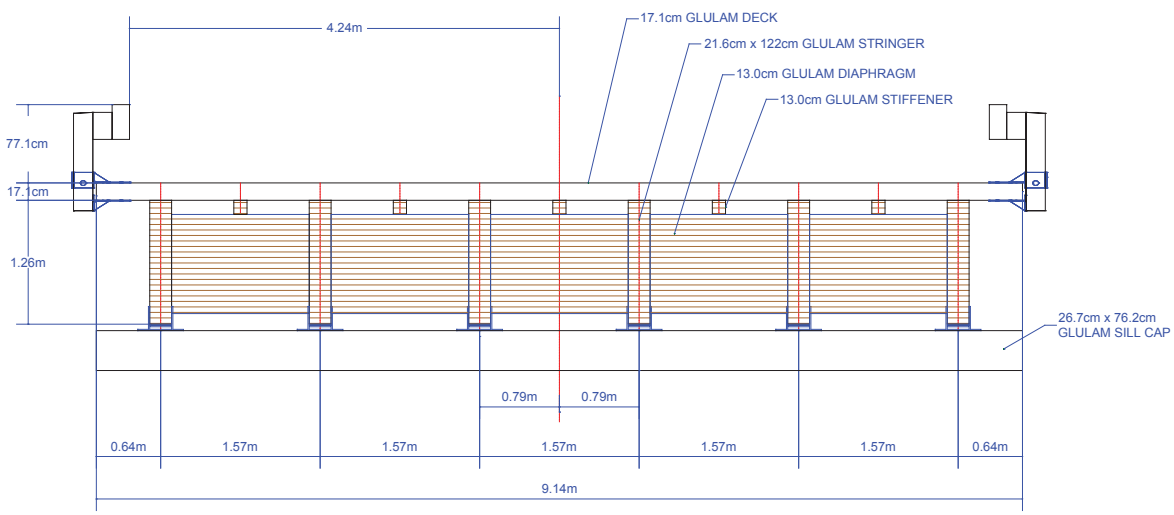

Fig. 3 The bridge cross section showing the configuration of the girders, the deck, and the Test Level 2 crash-tested guardrail system

Design of the GRS timber bridge is a direct reflection of current design practices for timber bridge construction in the United States. Out of the many styles and configurations of timber bridge superstructures, a glulam stringer design with glulam transverse deck panels was selected.

Timber stringers offer economic advantages compared with other design types but require consideration for things such as vertical clearance (that is, hydraulic opening in this case) as timber stringers often require deeper sections than their concrete and steel equivalents. The 16-m length of the GRS–IBS abutment supported superstructure is in an optimal span range for glulam stinger

bridges, and adjustments were made at the roadway approaches to accommodate the superstructure depth.

To minimize possible reflective cracking in the wearing surface, longitudinal timber stiffeners were used at midspan of the stinger spacing. These stiffeners were bolted to the underside of the transverse decking to assist in transferring differential deflections from panel to panel. Using stiffeners in conjunction with a waterproofing wearing surface has proven to maintain the stability of the decking and resist movements that otherwise resulted in the asphalt wearing surface cracking. To meet current safety performance standards, a Test Level 2 crash-tested, bridge railing system was installed that includes glulam posts and glulam railings but without a curb system. A bituminous asphalt wearing surface will be installed on the bridge roadway and approaches in the near future.

4. Structural Health Monitoring

4.1 Substructure Monitoring

The stability of GRS is one of its valuable aspects. Motion of the soil decreases the utility of the GRS structure. To date, monitoring of the movement of GRS–IBS abutments has come from manual surveying of set locations on the exposed side and top of the facing elements, the top of the abutment or the integrated approach, and the superstructure and comparing those points against fixed survey targets away from the bridge and abutments. The surveying data are typically collected manually at intervals of days, weeks, or months. Specific areas of interest within the GRS abutment are targeted for monitoring: movement or tilting of the back wall and wing walls, settlement at the superstructure sill and approach roadway joint, lateral soil movement within the GRS abutment, and soil pressure in high stress areas of the GRS abutment, which are subject to scour.

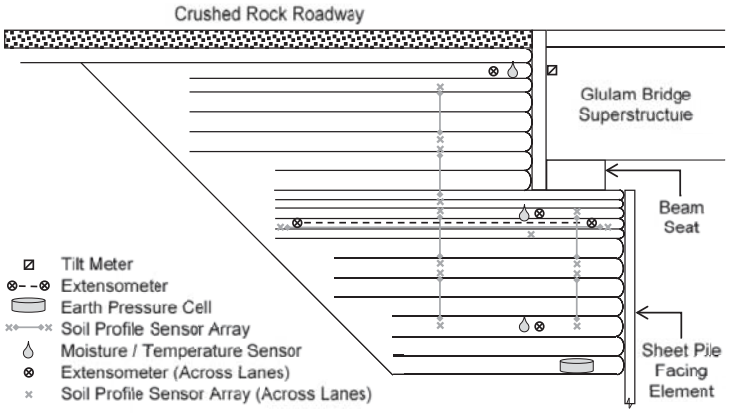

Fig. 4 Sensor placement within GRS abutment. Adapted from site design plans prepared by Buchanan County, Iowa, and used with permission

The monitoring sensors installed within the abutment are shown in Figure 4. The cross section shown in Figure 4 was adapted from the abutment design plans for the site and used with permission from Buchanan County, Iowa. The sensors include tilt meters, moisture and temperature sensors, extensometers, earth pressure cells, and soil profile sensor arrays. The tilt meters measure back wall and wing wall tilt angle. Vertically oriented extensometers (VE), referred to as borehole extensometers, measure abutment settlement. Each VE was approximately 58 cm long prior to installation. There are six sets of VE in the abutment. Four sets of two VE are positioned under the beam seat, 30 cm from the sheet pile facing element. Two sets of four VE are positioned within the roadway approach to the superstructure, 1.88 m from the facing element. Horizontally oriented extensometers (HE), referred to as soil extensometers, measure lateral soil movement. Four HE are used in total. Each HE was approximately 3.35 m long prior to installation. A set of two HE are positioned parallel to the roadway and placed near the midpoints of each of the two driving lanes. A set of two HE are positioned perpendicular to the driving lanes below the interface between the bridge and the approach. Soil profile sensor arrays (SPA), also referred to as shaped accelerometer arrays, and are a series of accelerometers connected by segmented rods. The rods are 0.5 m long. The connection points between the rods are hinged to allow a degree of freedom of motion between the rods. The accelerometers monitor relative movement at each of the connection points, providing internal soil profile information. Two sizes of SPA were used, 3 and 7 m. Two 3-m SPA were placed parallel to the roadway and near the midpoints of each of the two driving lanes. Three 7-m SPA were placed perpendicular to the driving lanes. The first was near the bottom of the abutment, approximately 1.37 m below the level of the beam seat and positioned directly below the interface between the approach and the superstructure. The second was placed at

approximately 25 cm below the level of the beam seat and directly below the interface between the approach and the superstructure. The third was placed near the top of the abutment, approximately 46 cm below the roadway surface and within the approach, 30 cm from the superstructure. Three moisture–temperature sensors were placed at the midpoint of the roadway 15 cm adjacent to each of the 7-m SPA as shown in Figure 4. Two earth pressure cells were placed at the bottom of the abutment, near the midpoints of each of the driving lanes and directly under the beam seat. Two sets of two tilt meters were affixed to the abutment back wall. Tilt meters measure tilt angle in one direction. The tilt meters were mounted in pairs of two and oriented such that the direction of angle measurement was perpendicular within each pair. The pair of tilt meters measure the angle of tilt of the back wall parallel and perpendicular to the driving lanes.

Several ambient condition sensors were mounted in and around the abutment. Wind speed, wind direction, solar radiation, and precipitation are measured on site. Temperature and relative humidity are measured on site, both above the level of the abutment and below the superstructure. The ambient condition sensors and datalogger housing are shown in Figure 5. The abutment and ambient condition sensors are summarized in Table 1. Data are collected from the abutment and ambient conditions sensors every 30 minutes by a CR1000 datalogger (Campbell Scientific, Inc., Logan, UT). The data are transmitted via cellular connection for processing and permanent storage.

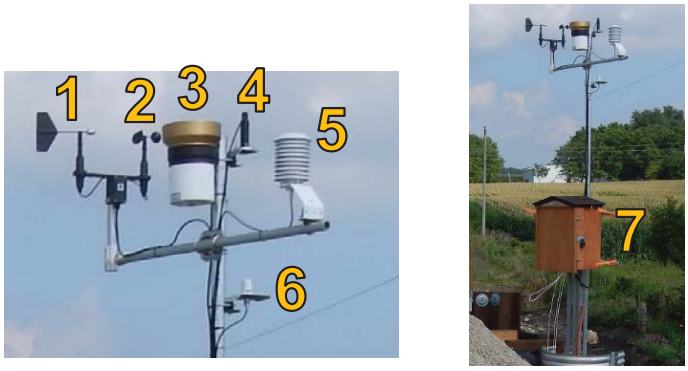

1. Vane
2. Anemometer
3. Tipping Bucket Rain Gage
4. Pyranometer
5. Temperature–Relative Humidity Probe
6. Cellular Antenna
7. Datalogger Housing

Fig. 5 Ambient weather condition sensors and datalogger housing

Table 1. GRS abutment and ambient weather condition sensor summary

Measuring	Sensor	Model	Quantity	Buried
Vertical Settlement	Extensometer	Geokon A3 w/ Model 4450 Transducer	16	Y
Back Wall Movement	Tilt Meter	Geokon 6350	4	Y
Soil Pressure	Earth Pressure Cell	Geokon 4800	2	Y
Horizontal Soil Movement	Extensometer	Geokon 4435	4	Y
Moisture–Temperature	Water Content Reflectometer	Campbell Scientific CS655	3	Y
Settlement Profile	Soil Profile Sensor Array	Measurand SAAF	5	Y
Wind Speed	Anemometer	03101 R.M. Young Wind Sentry	1	N
Wind Direction	Vane	03301 R.M. Young Wind Sentry	1	N
Solar Radiation	Pyranometer	Campbell Scientific SP230	1	N
Precipitation	Tipping Bucket Rain Gage	TE525	1	N
Temp–Relative Humidity	Temp–RH Probe	Rotronic HygroClip2	2	N

4.2 Superstructure Monitoring

The bridge superstructure is monitored with two independent SHM systems under dynamic loading, both triggering a 10-second window of data collection. The first system is based on strain measurements; the second system is based on force and displacement measurements.

4.2.1 Strain-Based Measurement Systems

The foundation of the instrumentation plan and monitoring system for the glulam superstructure is a modification of the BECAS monitoring system developed by ISU–BEC [7]. BECAS was initially developed for steel and concrete bridges for long-term, real-time monitoring situations and has been

successfully implemented on four interstate bridges in Iowa and Wisconsin. The system was first modified and tested on a glulam girder superstructure in Delaware County, Iowa, in 2012 [8]. After monitoring and fine-tuning that system for several years, minor changes and improvements were made prior to implementing the system on the bridge of this project.

The two main objectives of the SHM system on this bridge were to (1) collect structural performance data from the bridge and (2) provide real-time, continuous load rating of the superstructure for damage and deterioration detection. The SHM system for the GRS timber bridge consists of 36 strain gages installed on the glulam girders, 6 strain gages installed on the underside of the transverse glulam deck panels, 3 moisture sensors (2 in girders, 1 in deck) [9], and 2 temperature sensors. All 47 of these sensors are connected to and monitored by a CR9000X datalogger (Campbell Scientific). Figure 6 illustrates the instrumentation layout for the GRS timber bridge. An on-site desktop computer collects the data from the data logger and pushes them wirelessly via cell modem and router to the BEC main servers at the home office in Ames, IA. Figure 7 illustrates the logger enclosure mounted on the wingwall of the bridge. After the data are received by the servers, they are filtered and reduced, separating out data files with a detected truck event for further analysis and evaluation.

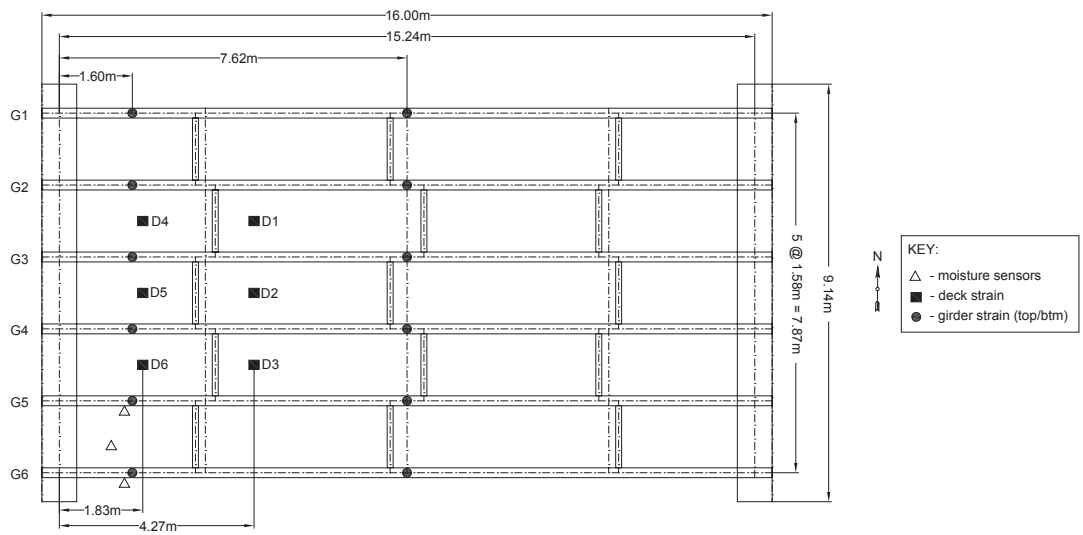

Fig. 6 GRS timber bridge instrumentation layout

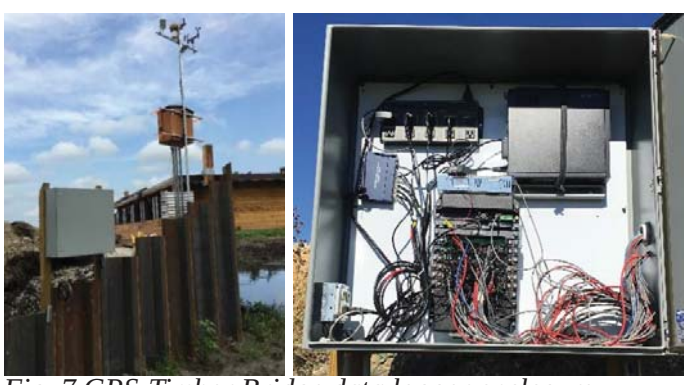

Fig. 7 GRS-Timber Bridge data logger enclosure

Girder strains are being collected at two cross sections: (1) a distance *d*, *d* being the depth of the girders, from the center of bearing of the girders at the west abutment, and (2) at midspan of the bridge as shown in Figure 6. Girder strain gages were installed approximately 5.1 cm below the deck surface and midwidth on the bottom of the girders at each location. As shown in Figure 8, each strain gage is comprised of a foil strain gage affixed to a 2.5- by 20.3-cm. strip of 0.127-mm-thick stainless steel. This strain gage configuration was developed in a previous research project by ISU and is referred to as a shim gage. The shim gage is then attached to the glulam girder using Loctite 426 adhesive (Loctite, Düsseldorf, Germany). Girder strains are used for multiple analyses of the structure, including but not limited to, the neutral axis, peak tensile strain, girder end rotation, transverse load distribution, and various truck detection–evaluation calculations.

Deck strains are collected at key locations, using the same shim gage configuration discussed previously, to obtain vehicle information as well as deck performance measures. The six deck gages

are located in bays 2, 3, and 4 and along two cross sections. As shown in Figure 6, the first cross section is located 1.83 m from the centerline of the girder bearing on the west abutment, and the second is located 2.44 m east of the first line. In each of the three instrumented bays, there is one strain gage per cross section located adjacent to the longitudinal stiffener beams and oriented in the transverse direction. The deck gages allow the BECAS system to not only detect the presence of a vehicle, but determine the speed of the vehicle, the transverse position of the vehicle on the bridge, the number and spacing of axles on the vehicle, as well as assess glulam deck performance.

Fig. 8 Shim gage configuration for measuring strains

The raw strain data collected in the SHM system are continuously stored in the database as 1-minute data files. Each 1-minute data file contains five strain components: (1) creep- and shrinkage-induced strain response; (2) temperature-induced strain response; (3) noise; (4) quasi-static strain response caused by ambient traffic; (5) dynamic strain response caused by ambient traffic and other dynamic loads such as wind. For this study, damage detection and structural capacity evaluation are both based on the quasi-static bridge response caused by truck events, which is a portion of strain component (4). Accordingly, the other four strain components are excluded from the strain data collected for these truck events. Truck events are identified using the deck strains; data files not found to have a truck event are discarded, and only data files representing truck events are further analyzed. A typical strain response to the presence of a three-axle truck crossing a bridge with an SHM system is shown in Figure 9.

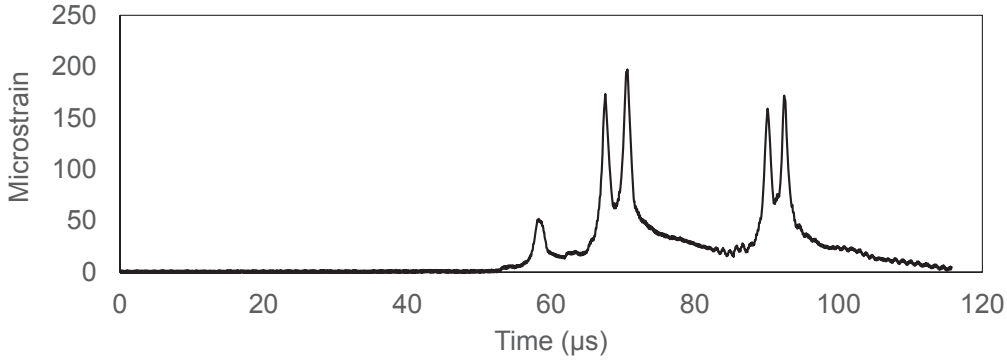

Fig. 9 Typical strain response of a three-axle truck crossing a bridge with an SHM system

The change of the strain response caused by creep, shrinkage, and temperature changes within a 1-minute period are considered negligible and can be neglected during the data process, which was also discussed by Doornink et al. [10] and Lu [7] . However, the strain response caused by creep, shrinkage, and temperature changes, which is almost constant in each data file, needs to be eliminated. To zero the strain response, a constant baseline strain should be determined for each strain sensor. The baseline strain for each sensor can be identified by finding the mode of the sensor data, which represents the value most frequently occurring in the 1-minute data collection [7]. The raw strain data of each sensor can then be zeroed with respect to the baseline strain to eliminate the creep-, shrinkage-, and temperature-induced strain components.

4.2.2 Force and Displacement Measurement Systems

The approach taken for monitoring the superstructure dynamic behavior is to consider that the superstructure is a black box composed of structural governing equations with unknown parameters that takes in first-order inputs in the form of forces and yields displacements as first-order outputs. Forces are measured using LBM-20K load cells (Interface, Inc., Scottsdale, AZ) capable of measuring up to 89.0kN. Two load cells are placed at each end of the six glulam stringers, for a total of 24 force measurements. A welded plate bearing assembly to which the load cells are

mounted and which affixes stringers to the beam seat is shown in Figure 10. The use of two load cells per stringer end ensures static equilibrium and facilitates measuring stringer torsion. Load cell signals are conditioned and digitized using six-input LabJack T7 Pro multifunction DAQ devices; four LabJack devices are utilized in all. Force measurement data is transferred from the LabJack via USB to a Raspberry Pi 2 single-board computer, which transmits the information to the remote server for archiving.

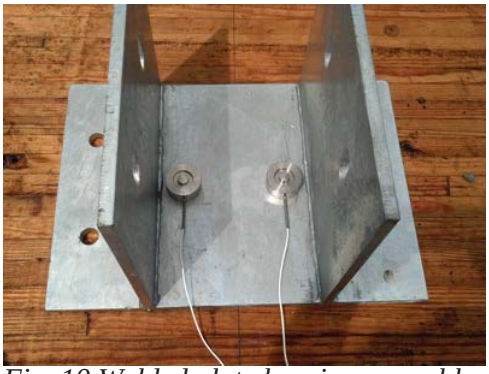

Fig. 10 Welded plate bearing assembly with mounted load cells

The displacement output of the bridge is measured by fixed reference frame cameras monitoring the movement of infrared laser LEDs. The LEDs are to be placed by identifying the locations on the bridge that provide the most robust and unique information to solve for the unknown parameters. The LED locations are determined by simulation of the superstructure behavior. The infrared laser LEDs have a divergence of 2° and are imaged using the camera settings as a white dot in a black background. The centroid of this dot is tracked in real time to monitor the movement of the bridge with subpixel accuracy. Two types of cameras are used to monitor the bridge. A Raspberry Pi NoIR Camera is attached to each of the four Raspberry Pis. The Raspberry Pi converts the image of the LED to a digital coordinate. The other camera system used is the Pixy CMUcam5. The Pixy camera system utilizes an embedded microcontroller to calculate the image to coordinate conversion onboard at 50Hz. The Raspberry Pi reads the coordinates output from the Pixy. The displacement data is sent with the force data to the server. An additional Raspberry Pi is utilized to act as a master to coordinate the timing between the four data acquisition Pis and to serve as a gateway between the locally networked Pis.

The generated force displacement data will be utilized to inversely solve for the unknown superstructure parameters by satisfying the governing system of equations. Each vehicle becomes an excitation to the system that adds to the behavior space for which to characterize the black box and which to subsequently compare against for indications of degradation.

5. Results

5.1 Girder Stiffness Testing

Fig. 11 Girder with weight at midspan during stiffness testing

To obtain a better understanding of the individual strength parameters of the girders for the bridge, and to facilitate more accurate modelling, calibration, and load ratings from the SHM system, all six glulam girders were individually load tested prior to installation at the bridge site. Testing took place at the Buchanan County maintenance shop. Each girder was positioned on temporary supports, set at the same distance as the abutments on the bridge, and braced laterally at each end. Three displacement transducers were then attached to the underside of the girder, one offset from each support approximately 2.5 cm, and another at midspan of the girder. Loading of the girders was achieved using a crane and the steel hammer from a pile-driving apparatus as dead weight. Total weight of the hammer and rigging was approximately 10.14 kN. Once the girders were properly braced, instrumented and data collection was underway, the weight was carefully, without impact, placed at midspan of the girder until full relief of tension in the crane rigging was achieved. Figure 11 illustrates a girder with the weight placed at midspan. Data was collected for approximately 10 sec. and then the weight was removed while data continued to be collected. Data collection was stopped once the weight was completely removed and displacements appeared to balance back to zero. This process was done twice for each

girder to ensure repeatability of the data. Using basic fundamentals from mechanics of materials and the data from the girder load tests, the Young's Modulus of each girder was calculated and is presented below in Table 2.

Table 2. Young's Modulus (GPa) for GRS Timber Bridge Girders

Girder	1	2	3	4	5	6
Test 1	9.03	9.10	8.62	9.51	10.00	11.38
Test 2	10.41	11.38	6.89	10.76	9.93	11.72
Average	9.72	10.27	7.79	10.14	10.00	11.58

5.2 GRS Settlement Measurements

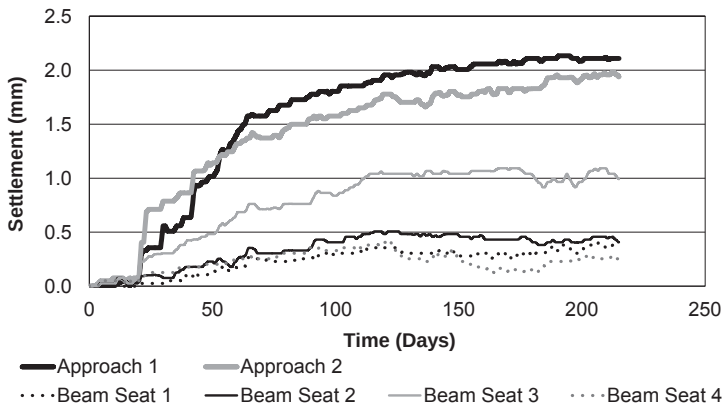

Fig. 12 Monitored settlement measurements from vertical extensometers mounted under the beam seat and within the roadway approach

As previously noted, the main benefit of the GRS-IBS system is the reduction in settlement of the approach roadway adjacent to the bridge ends. Settlement at the site is monitored by vertical extensometers (VE) installed into the abutment. The settlement results for the first 215 days of monitoring are given in Figure 12. The VE in the roadway approach are labelled Approach 1 and 2. The settlement for the approach is approximately 2 mm across a 2.32 m span (4 VE in series). The VE under the beam seat are labelled Beam Seat 1 through 4. The largest of the settlement measurements under the beam seat was Beam Seat 3, which has approximately 1 mm of settlement across a 1.16 m span (2 VE in series). Wahls indicated that a differential settlement of 12 mm would likely require maintenance, but would not be considered intolerable. The differential settlement between the roadway approach and the beam seat after 215 days is between 1 and 1.5 mm, far below the level requiring maintenance [11].

5.3 On-Site Validation Testing

In addition to the long-term structural monitoring being conducted by the SHM system, routine short-term live-load tests are included in the program for this structure. The initial load test will be conducted in the spring of 2017, with subsequent tests to follow every 6 to 12 months for a period of 2 to 3 years. These tests will involve use of a structural testing system and instrumentation from Bridge Diagnostics, Inc. (BDI) (Boulder, CO) and will allow for collection of strain and deflection data in addition to data collected by the on-site SHM system. BDI strain transducers will be installed in the proximity of the existing shim gages. In addition, deflections will be measured at midspan of each of the girders. Loading of the structure will be completed using loaded trucks, of known but varying weights and axle configurations, traveling across the bridge at crawl speed to collect quasi-static response data. Data from the live-load testing will be used to validate strains collected from the SHM system, verify vehicle recognition parameters for the system, and provide additional structural performance information on the structure. In addition to the structural-related measurements, moisture readings will be taken during the live-load testing using typical moisture meters to validate moisture readings collected by the SHM system.

6. Summary and Recommendations

A collaborative bridge design and construction effort culminated with the October 2016 opening of the Catt Bridge in Buchanan County, Iowa. The new bridge is supported by a nontraditional substructure system referred to as a geosynthetic reinforced soil (GRS) bridge abutment. The superstructure spans 16.2 m and is comprised of glulam girders supporting a transverse glulam deck

system. Both the sub- and superstructural systems are being actively monitored with an extensive array of sensors embedded in the GRS abutments or attached to the bridge superstructure. Data collected will be helpful in maintaining the overall health of the bridge by detecting structural deficiencies or triggering timely maintenance actions. This should result in a significant increase in the bridge's life expectancy, which could potentially exceed 100 years.

7. Acknowledgements

The authors thank the following individuals and organizations, who have contributed to the overall success of this project: Federal Highway Administration, Washington, DC; Laminated Concepts, Inc., Big Flats, New York; Alamco Wood Products, Albert Lea, Minnesota; and Brian Keierleber and the Buchanan County Bridge Team, Independence, Iowa. Special thanks are given to FPL electronics and computer engineers, Dave Simpson and Will Kinney, for their assistance with the installation of the field data acquisition system and weather station equipment.

8. References

[1] USDOT, Federal Highway Administration, National Bridge Inventory, January 2017, https://www.fhwa.dot.gov/bridge/nbi.cfm.

[2] Phares B. M., Wipf T. J., Deza U., Wacker J. P., *Development of a Smart Timber Bridge—A Five-Year Plan*, General Technical Report FPL-GTR-195, U.S. Department of Agriculture, Forest Service, Forest Products Laboratory, Madison, WI, 2011, 10 p.

[3] AASHTO, AASHTO M43, *Standard Specification for Sizes of Aggregate for Road and Bridge Construction*. American Association of State Highway and Transportation Officials, Washington, DC, 2005.

[4] AASHTO, AASHTO M288, *Standard Specification for Geotextile Specification for Highway Applications*, American Association of State Highway and Transporation Officials, Washington, DC, 2015.

[5] Adams, M., et al., *Geosynthetic Reinforced Soil Integrated Bridge System, Interim Implementation Guide*, No. FHWA-HRT-11-026, U.S. Federal Highway Administration, 2011.

[6] AASHTO, *Load and Resistance Factor Design (LRFD) Design Specifications for Highway Bridges*. 14th Edition. American Association of State Highway Transportation Officials, Washington, DC, 2014.

[7] Lu P., Wipf T., and Phares B., *A Statistical Based Damage Detection Approach for Highway Bridge Structural Health Monitoring*, Ph.D. Dissertation, Iowa State University, 2008.

[8] Boechler A., Pence T., Hosteng T., and Phares B., *Development of a Smart Timber Bridge – Sensor Evaluation, Algorithm Methods and Identify Changes in Timber Bridge Stiffness, and Developing a Timber Bridge Rail Impact Detection System*, Institute for Transportation, Iowa State University, 2015.

[9] Pence T., Hosteng T., Phares B., and Wacker J., *Investigation of Moisture Sensors for Historic Covered Bridges*, Institute for Transportation, Iowa State University, 2014.

[10] Doornink J., Wipf T., and Phares B., *Monitoring the Structural Condition of Fracture-Critical Bridges Using Fiber Optic Technology*, Ph.D. Dissertation, Iowa State University, 2006.

[11] Wahls, H.E. *NCHRP Synthesis of Highway Practices 159: Design and Construction of Bridge Approaches.* Transportation Research Board, National Research Council, Washington, DC, 1990.

SAMHÄLLSBYGGNAD

BYGGTEKNIK

Conference proceedings, ICTB 2017, 3rd International Conference on Timber Bridges

Anders Gustafsson, RISE, Anna Pousette, RISE

Olle Hagman, LTU, Mats Ekevad, LTU

SP Rapport 2017:26